The therapeutic potential of exosomes derived from mesenchymal stem cells in experimentally induced hypertensive encephalopathy

Original Article

Asmaa Kattaia[1], Samia Adel Abd EL-Baset[1], Rehab Abdul-Maksoud[2] and Eman Mohamed[1]

[1]Department of Medical Histology and Cell Biology, [2]Department of Medical Biochemistry, Faculty of Medicine, Zagazig University, Zagazig, Egypt

ABSTRACT

Background and objectives: Cerebrovascular complications of hypertension are highly dangerous. In recent studies, exosomes have been widely used in several disease research areas, including hypertension research. Mesenchymal stem cells (MSCs) release high levels of exosomes. Therefore, we investigated the role of MSC-derived exosomes in alleviating hypertension-induced changes in the cerebral cortex of a rat model.

Methods: A total of 30 rats were assigned to control, hypertensive, and exosome-treated groups which received 100 µg MSC-derived exosomes total protein via tail vein. Tissue samples were examined for gene expression using real-time quantitative polymerase chain reaction (RT-qPCR) and light and electron microscopy.

Results and conclusion: BExosome treatment recovered blood vessels, neural cells and blood-brain barrier (BBB) alterations as verified by upregulated endothelial nitric oxide synthase (eNOS) and AMP-activated protein kinase (AMPK) mRNA, downregulated α-smooth muscle actin (α-SMA) mRNA, and enhanced angiogenic factors, miRNA-222 and Tie2 protein. Exosomes exerted anti-apoptotic effects by increasing Bcl-xl expression and decreasing caspase 3 protein levels in immune histochemical sections. The anti-inflammatory potential of exosomes was indicated by reduced IL-1β mRNA and microglia activation factor Iba1 protein levels. Neuronal protection was supported by upregulated miRNA-133b and calbindin D28K (CB) protein levels. Moreover, the astrocyte vascular feet protein aquaporin (AQP4) was downregulated. MSC-derived exosomes may be considered a novel strategy for treating cerebral hypertension complications

Key Words: Cerebral cortex, Exosomes, Hypertension, Rat.

List of abbreviations: MSCs: mesenchymal stem cells, **eNOS:** endothelial nitric oxide synthase, **AMPK:** AMP-activated protein kinase, **α-SMA:** alpha-smooth muscle actin, **CB:** calbindin D28K, **AQP4:** aquaporin, **EVs:** extracellular vesicles, **miRNAs:** microRNAs, **NIH:** National Institutes of Health, **PBS:** phosphate-buffered saline, **BP:** blood pressure, **SBP:** systolic blood pressure, **DME:** Dulbecco's Modified Eagle Medium, **FBS:** fetal bovine serum, **HG-DMEM:** high glucose-modified eagles' medium, **RCMB:** Regional Center of Mycology and Biotechnology, **real-time qPCR:** real-time quantitative polymerase chain reaction, **cDNA:** complementary DNA, **H&E:** hematoxylin and eosin stain, **Iba1:** ionized calcium-binding adaptor molecule 1, **DAB:** diaminobenzidine, **UCT:** ultra-cut, **SPSS:** Statistical Package for Social Sciences, ***p* value:** probability values, **SD:** standard deviation, **BBB:** blood-brain barrier, **NO:** nitric oxide, **VEGFR2:** vascular endothelial growth factor 2, **Ang:** angiopoietins, **IL-1β:** interleukin-1β, **IFNγ:** interferons, **miR-133b:** miRNA-133b.

Revised: 19 June 2022, **Accepted:** 02 July 2022

Corresponding Author: *Samia Adel Abd EL-Baset*, *Department of Medical Histology and Cell Biology, Faculty of Medicine, Zagazig University, Zagazig, Egypt,* **Tel.:** *+201003556228*, **E-mail:** *prof.dr.samiaadel@gmail.com.*

ISSN: 1110-0559, Vol. 6, No. 1. June, 2022.

INTRODUCTION

Globally, hypertension is a major cause of mortality [1]; however, despite many antihypertensive drugs, it is a complicated illness accompanied by poor recovery and limited effective therapeutic treatments that prevent most complications[2]. Cerebrovascular complications are among the most dangerous symptoms and include hypertensive encephalopathy with associated headache, vomiting, seizures, visual disturbance, coma and death[3]. Other complications include epilepsy[4] and stroke[5]. Approximately 90 % of individuals aged over 55 years have a high risk of hypertension[6].

In the last decade, mesenchymal stem cell (MSC) research has advanced the treatment of retinal[7], heart[8] and liver disease[9]. However, many challenges face MSC applications; cells are large, they cannot easily pass-through capillaries[10] and they may cause pulmonary embolism[11]. However, MSCs release extracellular vesicles (EVs)[12] and in particular, EVs from specific MSCs exhibit high stability, a low risk of immune rejection, an ability

 DOI: 10.21608/jmh.2022.145535.1100

to cross the blood-brain barrier (BBB) and good storage capabilities[13]. Therefore, many researchers have focused on EV rather than MSC applications[14].

EVs display variable sizes and range from hundreds of nanometers to a few microns. They include apoptotic bodies[15], ectosome/microvesicles[16] and small-size EVs (exosomes) (30 nm–100 nm)[17]. Exosomes are formed during endocytosis as late endosomes, which accumulate as intraluminal vesicles to form multivesicular bodies. Some are extruded to extracellular spaces as exosomes[18] and contain proteins, lipids, RNA and DNA from their original cells, which promote cross-talk and affect other cells via paracrine actions[17].

The most exciting elements of exosomes are microRNAs (miRNAs), which alter gene expression, proliferation and differentiation of neighboring cells[19]. These miRNAs are non-coding RNAs, which regulate different cell biological actions[20].

Some molecules involved in vascular regulation are targeted by several miRNAs. Their downregulation may mediate endothelial cell dysfunction by affecting endothelial nitric oxide synthase (eNOS), angiogenesis, or inflammatory marker expression leading to hypertension complications[21].

Culture medium modifications also influence exosome effects inside recipient cells. When exosomes from MSCs are placed in hypoxic culture medium, they improve cardiac regeneration by increasing angiogenesis and perfusion in the infarct area of a myocardial infarction model[22]. A COVID-19 study reported that exosomes extracted from MSCs alleviated oxygen saturation in patients, decreased cytokine storms and improved immunity[23]. Many studies have also investigated exosomes as a means to increase autophagy and hence cryoprotection[24].

Exosomes are used also in diagnosis of some diseases such as renal ischemia/reperfusion injury and other urogenital diseases by detecting exosomes and their mRNA in urine[25]. Moreover, exosomes can be used as vehicles and nano-carriers for drug transport into target cells[26].

As MSCs release high levels of exosomes when compared with other body cells, we investigated this unique trait toward alleviating hypertension-induced changes in the cerebral cortex of rats.

MATERIALS AND METHODS

Study animals:

A total of 30 adult healthy male albino rats (12–14 weeks, weighing 180–200 g) were housed in the Breeding Animal House of the Faculty of Medicine, Zagazig University, Egypt. Animals were housed in plastic cages with filter tops in an artificially illuminated room in a light/dark cycle at a controlled temperature of 23°C ± 1°C and 55 % ± 5 % humidity. Animals were kept away from any potential chemical contamination and had ad libitum access to food and water. Rats were humanely cared for in accordance with Ethical Committee guidelines from Zagazig University and the National Institutes of Health (NIH) Guide for the Use and Care of Laboratory Animals. The study was approved by the Institutional Animal Care and Use Committee, Zagazig University, Egypt (Protocol approval number: 5929).

Experimental design:

After acclimatization for 1 week, rats were allocated into three groups. Group I (sham-operated, control group): ten rats underwent surgical procedures similar to group II, except the renal artery was not ligated.

Group II (hypertensive group): after 4 weeks of documented hypertension (see below), ten rats were injected with 0.5 ml phosphate-buffered saline (PBS) (exosome vehicle) through the tail vein, once/day for 2 weeks.

Group III (exosome-treated group): ten rats underwent the same surgical technique as group II, 4 weeks after documented hypertension and received 100 µg (total protein) MSC-derived exosomes in 0.5 ml PBS through the tail vein, once/day for 2 weeks[27].

Hypertension induction:

Hypertension was induced using a two-kidney one-clip procedure. Rats were anesthetized using intraperitoneal pentobarbital sodium (50 mg/kg) injections. The left renal artery was exposed via retroperitoneal flank incision, detached from the renal vein and then ligated using a nylon suture and the incision closed[28]. Blood pressure (BP) was assessed via the tail cuff technique using a

small rodent BP analysis system according to the manufacturer's instructions (Hatteras Instruments, NC, USA). Systolic blood pressure (SBP) was consecutively measured three times with < 5 mm Hg variance. The mean measurement was taken as the effective SBP value. Rats with SBP > 160 mm Hg were hypertensive[29].

Preparation of MSC-derived exosomes:

Exosome isolation was performed using MSC supernatants as conditioned media. Cells were rinsed in PBS and cultured in Dulbecco's Modified Eagle Medium (DMEM) plus 10 % exosome-depleted fetal bovine serum (Sigma-Aldrich, St. Louis, MO, USA). After incubation for 48 h, correspondent volume of culture medium conditioned by an equivalent number of cells was amassed and exosomes segregated at 4°C. The medium was then centrifuged at 300 × g for 10 min, 2000 × g for 10 min and 10,000 × g for 30 min to remove cells. Exosomes were pelleted by ultracentrifugation at 100,000 × g for 70 min, washed in cold PBS and re-ultracentrifuged at 100,000 × g for 70 min. Finally, the exosome pellet was resuspended in PBS[30].

Exosomes were quantified by measuring total protein concentrations using the micro Bicinchoninic Acid protocol (Pierce, Rockford, IL, USA)[31].

Characterization of MSC-derived exosomes:

Exosome labeling with PKH-26:

For exosome localization in cerebral tissue, PKH-26 (Sigma-Aldrich, St. Louis, MO, USA) was used. Exosome pellets were diluted to 1 ml in PKH-26 kit solution. Then, 2 µl fluorochrome was added to the suspension and maintained at 38.5°C for 15 min. Next, 7 ml serum-free high glucose-modified eagles' medium (HG-DMEM) was added to the suspension and ultracentrifuged at 100,000 × g for 1 h at 4°C. The final pellet was resuspended in HG-DMEM and stored at −80°C[32]. PKH-26-labeled MSCs from exosomes in cerebral cortex sections were traced using fluorescence microscope (Olympus BX50F4, No. 7M03285, Tokyo, Japan).

Transmission Electron Microscopy (TEM):

For TEM studies, 5 µl PBS was added to 5 µl exosomes and the mixture placed on Formvar/carbon-coated copper grids. After 45 min, grids were stained with uranyl acetate, flooded three times in PBS and left at room temperature[33]. Grids were examined and imaged using a JEOL TEM 1010 instrument (JEOL Ltd., Tokyo, Japan) in the Regional Center of Mycology and Biotechnology, Al-Azhar University.

Flow cytometry:

Surface antigen marker expression was examined using a FAC scan flow cytometer (Becton Dickinson, Heidelberg, Germany).

CD9 and CD63 (bone marrow MSC-derived exosome markers) expression was investigated; exosomes were incubated with antibodies against CD9 (1 / 50, Catalog No: M01202, BOSTER BIOLOGICAL TECHNOLOGY) and CD63 (1 / 10, Catalog No: ab108950, Abcam).

Sampling:

To verify vessels were free of blood, anesthetized rats were perfused in a trans-cardiac manner with 20 ml PBS. Then, rats were sacrificed by the intraperitoneal injection of pentobarbital (40 mg/kg). The brain was quickly removed and dissected into a right and left hemisphere. The right underwent histopathological analysis, whereas the left was immediately frozen in liquid nitrogen and stored at −80°C. Cortical blood vessel extracts were separated as previously described[34]. Isolated blood vessels were added to PBS and ultrasonically homogenized (Hielscher Ultrasonic Processor, Germany). Extracts were centrifuged for 10 min at 14000 × g (4°C). Then, extracts were stored at −80°C for real-time quantitative polymerase chain reaction (qPCR).

Molecular analysis:

Real-Time qPCR:

Total RNA was isolated from blood vessel extracts and the cerebral cortex using TRIzol reagent (Invitrogen, Carlsbad, CA, USA) following the manufacturer's instructions. RNA was reverse-transcribed to cDNA using the PrimeScript RT reagent kit (TaKaRa, Tokyo, Japan) according to the manufacturer and stored at −20°C.

Real-time qPCR was performed using SYBR Green qPCR mix (TaKaRa, Japan) on the ABI 7900 System (Applied Biosystems, Foster City, CA, USA). For miRNAs, U6 was used as an internal control for normalization. For mRNA, data were normalized against GAPDH.

The following primer sequences were used (Applied Biosystems): miR-133b, Forward: 5′-TTTGGTCCCCTTCAACCAGCT-3′ and

Reverse, 5′-GTGCAGGGTCCGAGG-3′; miR-222: Forward: 5′-ATCCAGTGCGTGTCGTG-3′ and Reverse: 5′- TGCTAGCTACATCTGGCT-3′; U6, Forward: 5′-CTCGCTTCGGCAGCACA-3′ and Reverse: 5′-AACGCTTCACGAATTTGCGT-3′; aquaporin (AQP4), Forward: 5′-GAAAACCCCTTACCTGTGG-3′; Reverse: 5′-AGCTGGCAAAAATAGTGA-3′; α-SMA, Forward: 5′-CCGACCGAATGCAGAAGGA-3′ and Reverse: 5′-ACAGAGTATTTGCGCTCCGAA-3′; eNOS: Forward, 5′-AGCATACCCCCACTTCTGTG-3′ and Reverse, 5′-GAAGATATCTCGGGCAGCAG-3′; AMPK, Forward: 5’-TGAAGCCAGAGAACGTGTTG-3’ and Reverse: 5′-ATAATTTGGCGATCCACAGC-3’; interleukin-1β (IL-1β), Forward: 5′-CACCTCTCAAGCAGAGCACAG-3 Reverse: 5′-GGGTTCCATGGTGAAGTCAAC-3; B-cell lymphoma-extra-large (Bcl-xl), Forward: 5′-TGGAGTAAACTGGGGGTCGCATCG and Reverse: 5′-AGCCACCGTCATGCCCGTCAGG; GAPDH, Forward: 5′-GAAGGTGAAGGTCGGAGT-3′ and Reverse: 5′-GAAGATGGTGATGGGATTTC-3′.

A 20 µl reaction volume contained: 10 µl 2 × SYBR Green PCR master mix, 2 µl cDNA, 10 µmol/l primer pairs and a final volume of ddH2O.

The miRNA amplification protocol consisted of an initial hot start at 95°C for 30 s, followed by 40 cycles of 10 s at 95°C, 30 s at 60°C and finally 10 s at 72°C. The mRNA amplification protocol included an initial denaturation step of 30 s at 95°C and then 40 cycles of 5 s at 95°C and 34 s at 60°C. All reactions were performed in duplicate. Relative mRNA and miRNA expression levels were determined using the 2-ΔΔCt method, where ΔΔCt = [(target gene) cycle threshold (Ct) - (reference gene) Ct] in the experimental group - [(target gene) Ct - (reference gene) Ct] in the control group.

Histopathology:

Light microscopy:

Hematoxylin and eosin (H&E) staining:

Specimens were fixed in buffered formalin (10 %) and 5-µm-thick sections were processed in H&E[35].

Immune histochemical staining:

Calbindin D28K (CB), ionized calcium-binding adaptor molecule 1 (Iba1), caspase 3 and Tie2 localization in cerebral tissue was performed using immune histochemical staining. The avidin biotin-peroxidase complex method was performed according to the manufacturer’s instructions (Peroxidase, Dako ARK, Code No. K3954, Dako, Glostrup, Denmark). Sections were incubated overnight with primary antibodies: CB (rabbit polyclonal antibody; 1 / 500; Catalog No. PA5 - 85669; Thermo Scientific, San Jose, CA, USA), Iba1 (goat polyclonal antibody; 1 / 1000; Catalog No: ab5076; Abcam, Cambridge, UK), caspase 3 (rabbit monoclonal antibody; 11000/; Catalog No; EPR18297, ab184787; Abcam) and Tie2 (rabbit polyclonal antibody; 1 / 100; Catalog No: ab218051; Abcam). Biotinylated secondary antibodies using labeled horseradish peroxidase, the chromogen, 3,3’-diaminobenzidine (DAB) were used to stain tissue antigen sites brown. Mayer’s hematoxylin was used as a counterstain. Primary antibodies were omitted from negative controls[36].

Electron microscopy examinations:

Specimens were fixed in phosphate-buffered glutaraldehyde (2.5 %, pH 7.4) and then osmium tetroxide (1 %, 4°C) in the same buffer. Dehydration was followed by embedding specimens in epoxy resin and a Leica ultra-cut instrument was used to cut sections that were stained in lead citrate and uranyl acetate[37]. Sections were examined and photographed by TEM (JEOL JEM 1010, JEOL Ltd.).

Morphometric studies:

A Leica QWin 500 image analyzer computer system (Leica Ltd., Cambridge, UK) was used for data analysis. The software was linked to an optical microscope (Olympus, Tokyo, Japan) with a digital camera. In immune-stained sections, cells positive for-CB, anti-caspase 3 and anti-Tie2 were enumerated. Positive anti-Iba1 percentages were also measured.

All measurements were performed at a magnification of 400× in 20 mm^2 frames. Using the interactive measurement menu, five non-overlying fields were randomly selected and analyzed from each animal in each group. Measurements were performed by a blinded investigator.

Statistical analysis:

Statistical Package for Social Sciences version 22 (IBM Corp., Armonk, NY, USA) was used for data analysis. Values were presented as the mean ± standard deviation (X ± SD). One-way

analysis of variance tests were followed by Tukey's post hoc tests. Probability values (p) < 0.05 were significant and highly significant at < 0.001.

RESULTS

Exosome characterization:

Exosomes were traced in cerebral cortical tissues using PKH-26 dye (Figure 1A). TEM showed a spheroid exosome morphology of 50 nm–100 nm in diameter (Figure 1B). Flow cytometry of cell surface exosome markers showed CD63 and CD9 expression (Figure 1C, D).

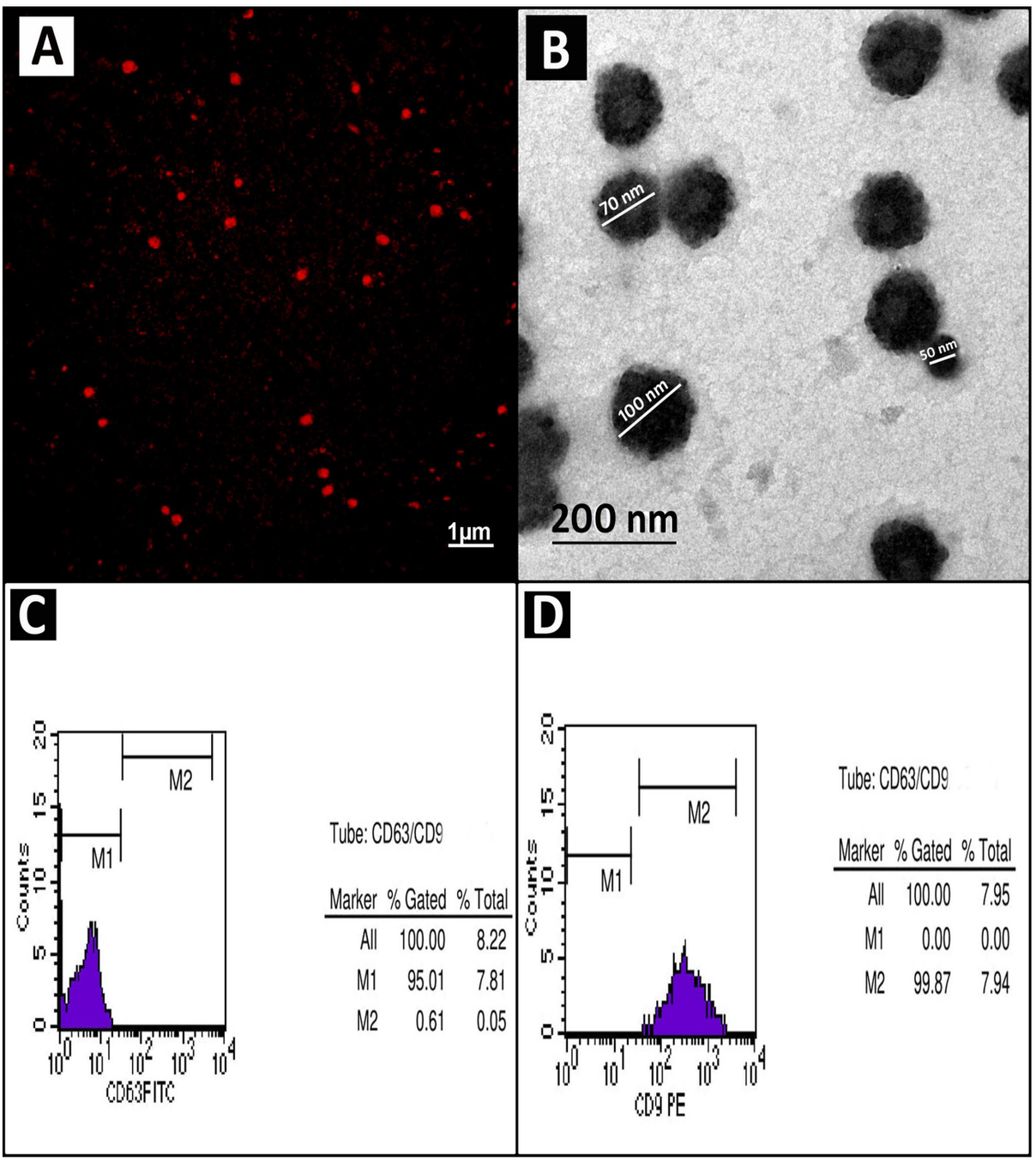

Figure 1: [A] A cerebral cortex section from the exosome-treated group showing PKH-26-labeled exosomes as bright red dots under fluorescence microscopy. [B] TEM showing spheroid-shaped exosomes with 50 nm–100 nm diameters. [C&D] Flow cytometer analysis showing the exosomal expression of the cell surface markers CD63 and CD9.

Real-time qPCR:

The hypertensive group showed highly significant decreases in miR-133b, miR-222, eNOS, AMPK, and Bcl-xl mRNA levels ($p < 0.001$) and highly significant increases in AQP4, α-SMA, and IL-1β ($p < 0.001$) levels when compared with controls. The exosome-treated group showed significant increases in eNOS ($p < 0.05$); highly significant increases in miR-133b, miR-222, AMPK, and Bcl-xl ($p < 0.001$) levels; and highly significant decreases in AQP4, α-SMA, and IL-1β ($p < 0.001$) levels when compared with the hypertensive group. In contrast, no significant differences were observed when compared with the control group ($p > 0.05$) except for eNOS and AMPK levels ($p < 0.05$) (Table 1).

Table 1: Real-time qPCR analysis of microRNAs and mRNA expressions:

	Control	Hypertensive	Exosome-treated group
miR-133b	1.05 ± 0.07	0.53 ± 0.11**c	0.96 ± 0.10**h
miR-222	1.08 ± 0.12	0.42 ± 0.11**c	0.89 ± 0.14*c, **h
AQP4	1.06 ± 0.11	2.51 ± 0.73**c	1.36 ± 0.27**h
α-SMA	1.15 ± 0.15	3.32 ± 0.53**c	1.57 ± 0.37**h
eNOS	1.02 ± 0.05	0.62 ± 0.15**c	0.83 ± 0.16*c, *h
AMPK	1.06 ± 0.06	0.37 ± 0.11**c	0.93 ± 0.11*c, **h
IL-1β	1.03 ± 0.06	2.74 ± 0.56**c	1.28 ± 0.24**h
Bcl-xl	1.01 ± 0.03	0.43 ± 0.11**c	0.87 ± 0.12*c, **h

miR-133b: microRNA-133b; miR-222: microRNA-222; AQP4: aquaporin 4; α-SMA: alpha-smooth muscle actin; eNOS: endothelial nitric oxide synthase; AMPK: adenosine monophosphate-activated protein kinase; IL-1β: interleukin-1β; Bcl-xl: B-cell lymphoma-extra-large. Values are listed as mean ± standard deviation (X ± SD); *: $P < 0.05$; **: $P < 0.001$; c: compared to the control group; h: compared to the hypertensive group; n = 10 animals.

H&E results:

Light microscope examination of H&E-stained sections of the control group showed that the cerebral cortex (frontal cortex) had a layered appearance and was formed of molecular, outer granular, outer pyramidal, inner granular, inner pyramidal, and multiform layers (Figure 2A). The pia mater was adherent and intact and molecular layers appeared compact and were formed mostly of glia and neuronal processes. Granule and pyramidal neurons, in the following layers, had open face nuclei and prominent nucleoli. Neuroglial cells with denser nuclei were scattered in compact neuropil. Blood vessels were surrounded by narrow spaces or "Virchow-Robbins spaces" (Figure 2B, C).

Hypertensive animals displayed swollen separated pia mater with large congested blood vessels and extravasated RBCs. The molecular layer displayed a vacant neuropil (Figure 2D). Areas of focal gliosis with inflammatory cell infiltrates were observed between cells (Figure 2E). Degenerated neuronal cells appeared irregular and shrunken with dark nuclei. They were enclosed in wide perineural spaces and contained vacuolated neuropil with congested blood vessels (Figure 2F). Many glial cells were surrounded by wide spaces, and degenerated neuronal cells and vacuolated neuropil were observed (Figure 2G).

Sections in the exosome-treated group showed the molecular layer and the inner layers of the cerebral cortex. Normal pia mater and molecular layers were observed. We also observed near-normal granule and pyramidal cells, except for few darkly stained cells within the tight neuropil. Blood vessels were enclosed in narrow perivascular spaces. Normal glial cells were also recorded (Figure 2H, I).

Immune histochemistry:

Immune histochemical stained CB sections in the control group displayed positive cytoplasmic immune reactions in most neurons (Figure 3A); reactions were identified in a few cells in the hypertensive group (Figure 3B), while the exosome-treated group showed positive reactions in many neuronal cells (Figure 3C). Anti-Iba1-stained sections of controls showed reactions in the soma and processes of few microglia (Figure 3D), while more immune-stained cells appeared in the hypertensive group (Figure 3E). Sections from the exosome-treated group showed few Iba1 positively stained cells (Figure 3F).

Control anti-caspase 3 immune-stained sections showed scant positive immune reactions (Figure 4A). Many positive immune-stained cells were observed in the hypertensive group (Figure 4B). In the exosome-treated group, few immune reactive cells were seen (Figure 4C). Immune histochemical Tie2-stained sections showed positive reactions in the endothelium of some cortical blood vessels (Figure 4D); reactions were markedly decreased in the hypertensive group (Figure 4E), while in the exosome-treated group, many positively stained vessels were identified (Figure 4F).

Morphometric results:

Statistical analysis of morphometric results in the hypertensive group showed a highly significant increase in the mean percentage area of positive immune reactions in anti-Iba1-stained sections and the mean number of positive cells in anti-caspase 3-stained sections. However, the mean percentage

area of anti-CB-stained cells and the mean number of anti-Tie2-stained vessels were significantly decreased when compared with controls. Conversely, the exosome-treated group showed a significant reduction in the mean percentage area of anti-Iba1-stained microglia and mean counts of anti-caspase 3-stained cells. Moreover, a significant enhancement in the mean percentage area of anti-CB-stained cells and the mean number of anti-Tie2-stained vessels was observed when compared with the hypertensive group (Figures 3G, H and 4G, H).

Ultrastructure results:

Electron microscopy of control group sections showed that blood capillaries were lined by smooth endothelial cells and pericytes with a thin basal lamina. Tight junctions between the endothelial lining were observed. Intact myelinated axons and mitochondria were also noted. Perivascular astrocytic processes contained gliofilaments and mitochondria. Junctional zones were distinct at the interface between neuronal membranes and astrocytes indicating intact BBB (Figures 5A and 6A). Neuronal soma showed euchromatic nuclei and dendritic processes. The perikaryon contained rough endoplasmic reticulum (RER) cisternae and free ribosomes, Golgi apparatus, and normal-density mitochondria. Compact neuropils were also seen (Figure 7A, B). Nerve fibers appeared either unmyelinated or myelinated with regular myelin lamellae. The axoplasm contained neurofilaments and mitochondria with intact cristae (Figure 8A).

Hypertensive group sections showed blood capillaries with disrupted endothelial lining, fenestrae, and long projections of the luminal membrane. Integrity loss in basal lamina and pericyte membranes were also seen (Figure 5B). Some blood capillaries were surrounded by swollen perivascular astrocytic processes, with increased cytoplasm translucence and organelle loss. Other swollen astrocytes exhibited increased cytoplasm translucence (Figure 6B). Blood capillaries had a relatively thickened basal lamina. Extravasated RBCs were also recorded indicating disrupted BBB (Figure 6C). Nerve cells showed irregular contours, dark muddy nuclei, irregular nuclear envelopes with dimples, dilated RER cisternae, and mitochondria-containing ruptured cristae (Figure 7C). Myelinated nerve fibers displayed sheath disruption, with split myelin lamellae and mitochondria-containing ruptured cristae (Figure 8B).

Exosome-treated group sections showed that some blood capillaries were lined by near-normal endothelial cells, except for some vacuoles and luminal membrane projections. Surrounding pericytes and thin basement membranes were noted (Figure 5C). Some blood capillary sections had a smooth endothelial lining and thin basal lamina. We observed astrocyte perivascular feet; they displayed gliofilaments and mitochondria. Most neurons were normal (Figure 6D) and most nerve cells appeared normal with euchromatic nuclei, RER profiles, ribosomes and normal mitochondria. The surrounding neuropil appeared normal (Figure 7D). Both unmyelinated and myelinated nerve fibers were identified; myelinated fibers were surrounded by regular myelin sheathes. Axons were filled with neurofilaments and mitochondria-containing normal cristae (Figure 8C).

A significant decrease in the body weight was detected in group II and group III as compared to normal rats. The body weight in group IV was significantly elevated as compared to the group II rats. There was no significant reduction in mean body weight between group IV and group I and between group IV with group III (Table 1).

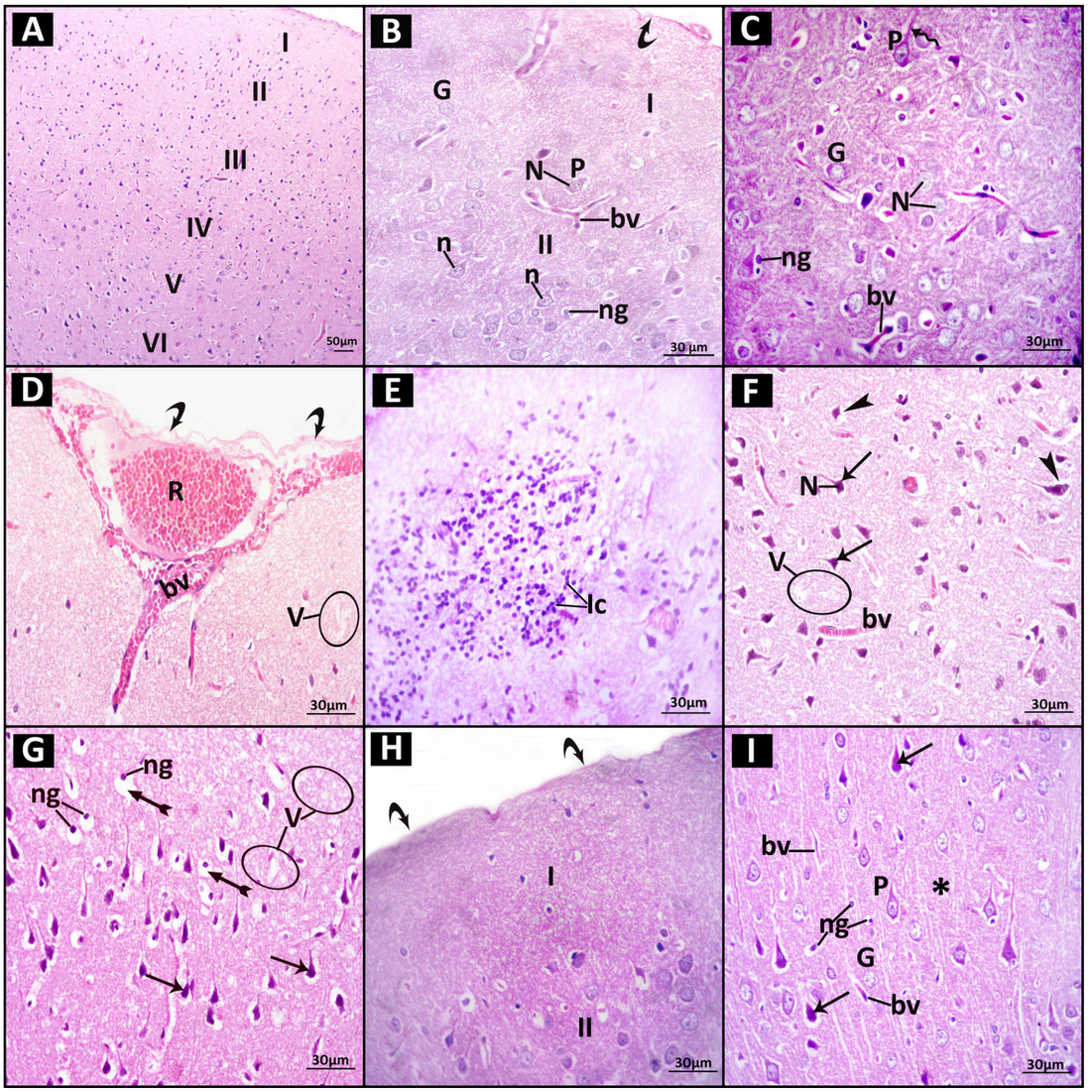

Figure 2: H&E-stained rat cerebral cortex sections in study groups [A–C]. Control groups. [A] The cerebral cortex (frontal cortex) shows a layered appearance; molecular (I), outer granular (II), outer pyramidal (III), inner granular (IV), inner pyramidal (V), and multiform (VI) layers. [B] The molecular layer (I) and outer granular layer (II). [C] Inner layers of the cerebral cortex. [B, C] The pia mater (curved arrow) is adherent and intact; the molecular layer appears compact and is formed mostly of glia and neuronal processes (zigzag arrow). Granule (G) and pyramidal neurons (P), in the following layers, have open face nuclei (N) and prominent nucleoli (n). Neuroglial cells (ng) with denser nuclei are scattered in compact neuropil. Blood vessels (bv) are surrounded by narrow spaces or "Virchow-Robbins spaces." [D–G] The hypertensive group. [D] Swollen separated pia mater (curved arrow) is shown with large congested blood vessels (bv) and extravasated RBCs (R). The molecular layer has a vacant neuropil (V). [E] A focal gliosis area with inflammatory cell infiltrates (Ic) is observed. [F] Degenerated neuronal cells (arrow) appear as irregular and shrunken with dark nuclei (N). They are enclosed in wide perineural spaces (arrow head) and vacant neuropil (V). Congested blood vessels are also seen (bv). [G] Many glial cells (ng) are surrounded by wide spaces (tailed arrow). Degenerated neuronal cells (arrow) and vacuolated neuropil (V) are also observed. [H&I] The exosome-treated group. [H] The molecular layer (I) and outer granular layer (II) appears with normal pia mater (curved arrow). [I] Inner cerebral cortex layers have near-normal granule (G) and pyramidal (P) cells, except for a few darkly stained cells (arrow) appearing within tight neuropil (asterisk). Blood vessels (bv) are enclosed in narrow perivascular spaces. Normal glial (ng) cells are also seen.

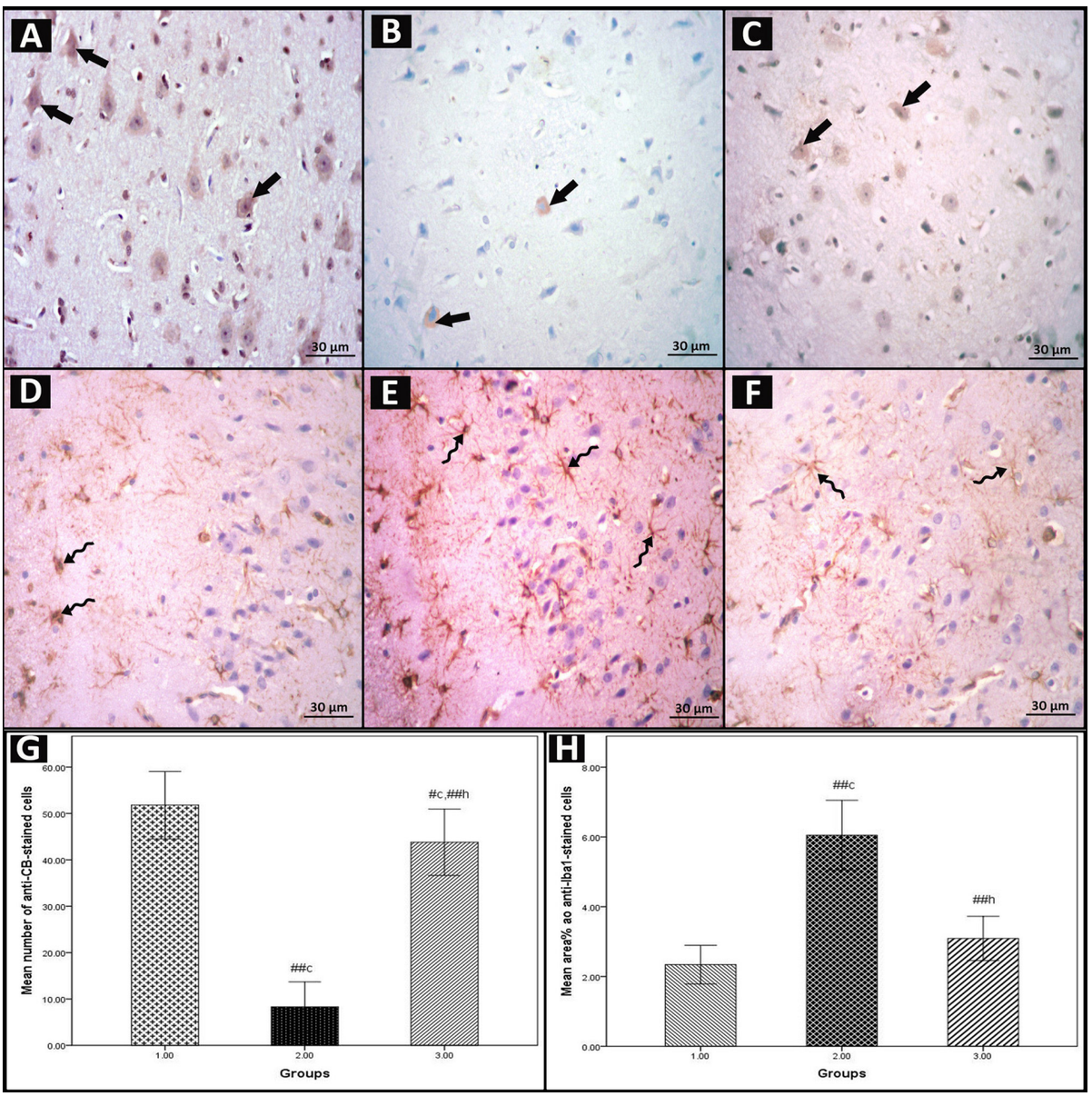

Figure 3: Immune histochemical stained rat cerebral cortex sections of the study groups. [A&D] control group, [B&E] hypertensive group, [C&F] exosome-treated group. [A–C] immune reactions for Calbindin D28k (CB) (thick arrow) in the cortical neurons. [D–F] ionizd calcium binding adaptor molecule 1 (Iba1) immune-reactions (zigzag arrow) in microglia. [G] the mean number of brown cells in anti-CB-stained sections; [H] the mean area % of positive microglia in anti-Iba1-stained sections. Values are displayed as mean ± standard deviation (X ± SD); C: *P* compared to control group; h: *P* compared to hypertensive group; #: $P<0.05$; ##: $P<0.001$.

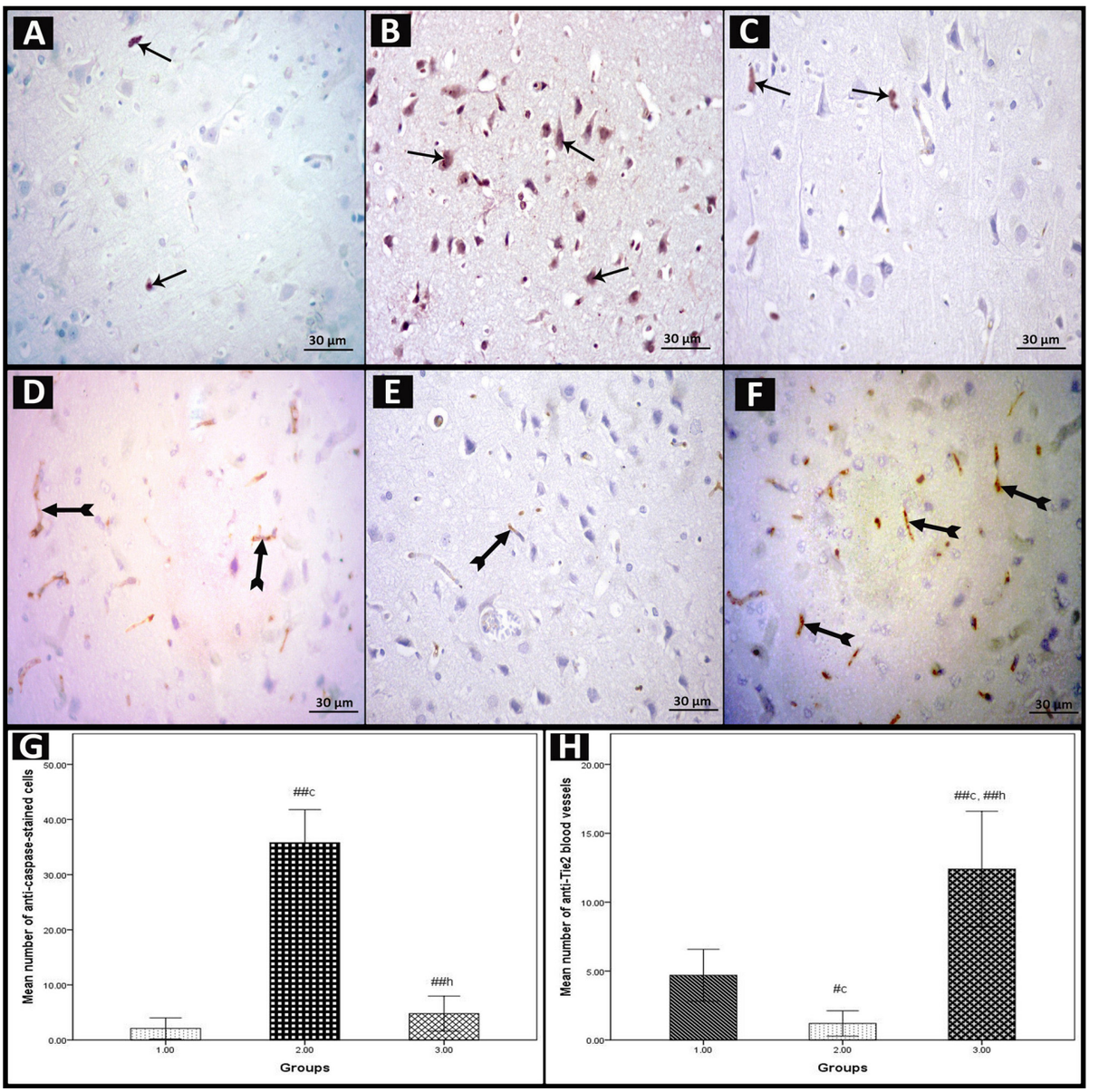

Figure 4: Immune histochemical stained rat cerebral cortex sections of the study groups. [A&D] control group, [B&E] hypertensive group, [C&F] exosome-treated group. [A–C] immune reactions for caspase3 (arrow) in the cortical neurons. [D–F] Tie2 immune reactions (tailed arrow) in cortical blood vessels. [G] the mean count of immune reactive cells in anti-caspase3-stained sections; [H] the mean number of positive blood vessels in anti-Tie2-stained sections. Values are displayed as mean ± standard deviation (X ± SD); C: P compared to control group; h: P compared to hypertensive group; #: $P < 0.05$; ##: $P < 0.001$.

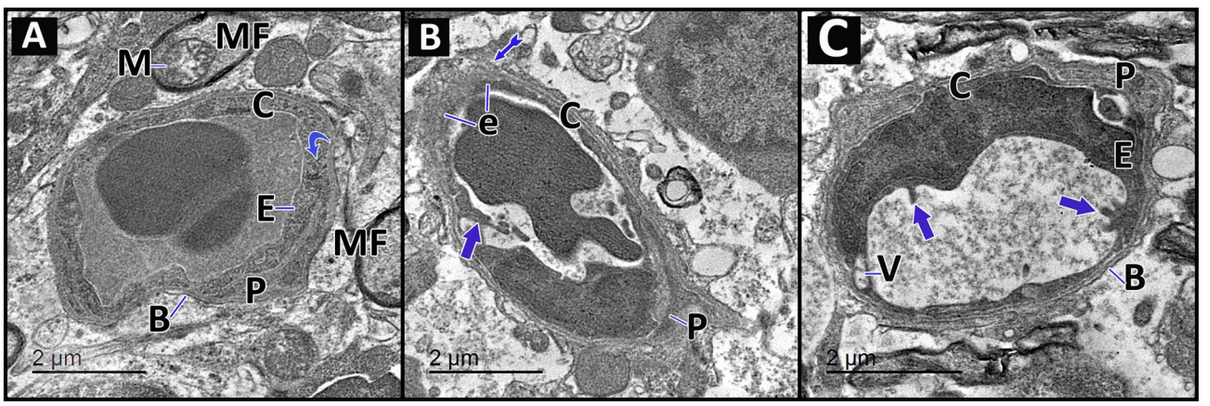

Figure 5: TEM rat cerebral cortex blood capillaries sections. [A] control group, [B] hypertensive group, [C] exosome-treated group. [A] A blood capillary (C) is lined by smooth endothelial cells (E) and pericytes (*P*) with a thin basal lamina (B). Tight junction (curved arrow) between the endothelial lining the blood capillary can be seen. Notice intact myelinated axons (MF) and mitochondria (M). [B] A blood capillary (C) shows disrupted endothelial lining (e) with fenestrae and long projections of the luminal membrane (thick arrow). Loss of integrity of basal lamina (tailed arrow) and the pericyte membrane (*P*) is also seen. [C] A blood capillary (C) is lined by nearly normal endothelial cells (E) except for some vacuoles (V) and projections of the luminal membrane (thick arrow). Note the pericyte (*P*) and the thin basement membrane (B).

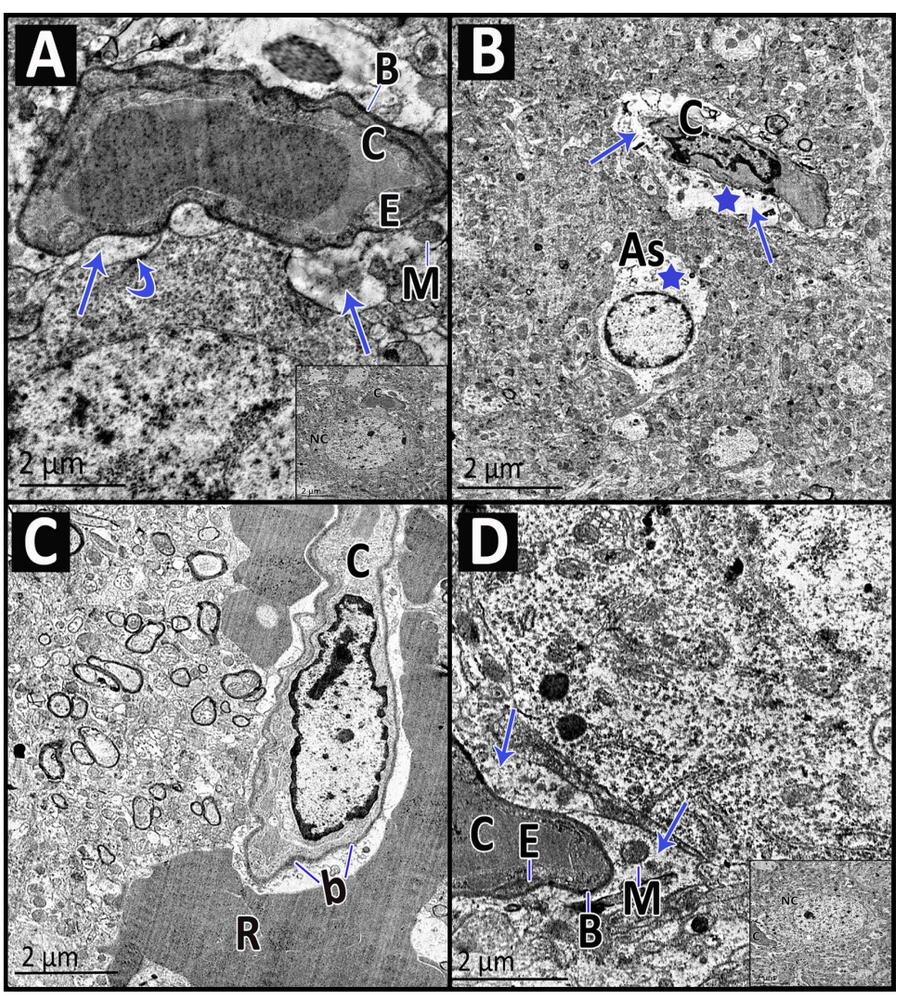

Figure 6: TEM rat cerebral cortex blood capillaries sections. [A] control group, [B&C] hypertensive group, [D] exosome-treated group. [A] A blood capillary (C) with regular endothelial lining (E), thin basal lamina (B) and perivascular astrocyte processes (arrow) containing gliofilamints and mitochondria (M). Junctional zones (curved arrow) are distinct at the interface between the neuronal membrane and astrocytes. Inset: the neuron (NC) is seen with a nearby capillary (C). [B] A blood capillary (C) is surrounded by swollen perivascular astrocyte processes (arrow) with increased cytoplasm translucence (star) and loss of organelles. A nearby swollen astrocyte (As) shows also increased translucence (star) of its cytoplasm. [C] A blood capillary (C) reveals relatively thickened basal lamina (b) of its endothelial lining. Extravasated RBCs (R) are also noticed. [D] A part of blood capillary (C) with smooth endothelial lining (E) and thin basal lamina (B). The perivascular feet of astrocytes (arrow) have glial filaments and mitochondria (M). Inset: the blood capillary(C) is seen in the vicinity of normal neuron (NC).

DISCUSSION

Hypertension is a growing health problem in the community[7]. In the past, researchers paid little heed to EV release from cells; however, the discovery that their biological content facilitated cross-talk between cells has meant a considerable increase in human disease research[38].

In this study, vascular vulnerability to hypertension was observed via congested blood vessels, extravasated RBCs, degenerated endothelial lining, pericyte disruption, thickened basal lamina, and swollen astrocyte perivascular feet. These alterations affected BBB integrity and contributed to its deterioration. In support of our results, Rapoport[39] reported that when intracranial pressure was massively increased, the BBB was broken and endothelial tight junctions were disrupted. Moreover, hypoperfusion to microvessels deprived endothelial cells of adequate oxygen, thereby affecting tight junction efficacy[40].

Significant eNOS downregulation was observed in hypertensive rats. Nitric oxide (NO) is produced by eNOS and has key roles regulating SBP, vascular tone, and angiogenesis. Notably, decreased eNOS expression reduced NO production, which compromised cerebral vessel dilation. eNOS also regulates neurogenesis, axonal growth, and synaptic plasticity in the cerebral cortex[41]. Cerebrovascular diseases are associated with decreased eNOS levels and a higher incidence of cognitive deficits[42]. We also observed a marked decline in AMPK mRNA expression in the hypertensive group. AMPK is an energy regulator and plays roles in brain hormonal signaling, glucose sensing, and neuronal integrity and function[43]. AMPK protects neurons from oxidative stress and metabolic disorders[44], whereas dysfunctional AMPK signaling pathway is correlated with various diseases involving hypertension[45].

We observed a significant increase in α-SMA mRNA expression in the vessel wall of hypertensive rats, consistent with Attwell *et al*.[46]. α-SMA is a cytoskeletal protein expressed in brain vessels with essential roles in vascular contraction and blood flow regulation[47]. When BP exceeds autoregulation limits, smooth muscle exhaustion occurs with forced dilatation. Consequently, autoregulation failure leads to brain edema and BBB destruction[48].

In this study, hypertensive exosome-treated rats showed almost normal blood vessel architecture. Exosome treatment upregulated eNOS and AMPK but downregulated α-SMA mRNA expression. These results agreed with Feng *et al*.[49] who reported that increased eNOS and AMPK levels in the endothelium of exosome-treated hypertensive rats reduced arterial stiffness. EVs exert antifibrotic effects by decreasing matrix metalloproteinase, transforming growth factor-β1, and elastase activity. EVs trigger endothelial cell angiogenesis by increasing vascular endothelial growth factor 2 phosphorylation[50]. We also observed miR-222 expression enhancement, which stimulated endothelial cell angiogenesis. Importantly, previous research provided insights on other exosome miRNAs responsible for angiogenesis, e.g., miR-21, let-7f and miR-181b5p/TRPM7[51].

Tie2 is a 140 kDa tyrosine kinase receptor present on endothelial cells, with roles in vascular stabilization and angiogenesis[52]. Angiopoietins (Ang) are blood vessel regulators that function by binding to Tie2 receptors, Ang-1/Tie2 signaling pathway has an anti-apoptotic effect in endothelial cells[53] and stimulates neural outgrowth[54]. In our study, a significant reduction in Tie2 immune expression was observed in hypertensive rats when compared with control and exosome-treated rats. In agreement with our results, Zhao *et al*.[55] reported a drop in the Ang-1/Tie2 system in pulmonary hypertensive rats. Yamamoto *et al*.[56] also suggested that increased vascular resistance and hypoxia led to Ang-1/Tie2 and VEGF downregulation with subsequent vascular rarefaction, blood vessel loss, and impaired angiogenesis, culminating in more vascular resistance and hypoxia. However, we revealed a significant elevation in Tie2 immune histochemical expression in exosome-treated rats suggesting increased angiogenesis and vessel wall stabilization. Similarly, Zhao *et al*.[57] indicated that MSC-derived exosomes stimulated lymphangiogenesis via the exosomal transfer of Ang-2/Tie2. Furthermore, exosomes derived from endothelial cells and MSCs were shown to secrete Angs[58]. High Ang-1 expression in the forebrain increased vascularization and dendrite formation in neurons[59].

Oxidative stress and inflammation are major causes of BBB impairment and neuronal destruction[60]. In our study, a robust increase in activated microglia was observed via the significant upregulation of Iba1 immune expression in hypertensive animals when compared with controls. Iba1 is a calcium-binding protein involved in cell ruffling and also phagocytosis in activated microglia, which is mediated by its actin-binding activity[61]. In hypertensive rats, enhanced mRNA expression of the inflammatory marker, interleukin-1β (IL-1β), was observed together with inflammatory cell infiltration. Inflammatory cells were distinguished

by Kaiser *et al.*[62] as natural killer cells that are attracted by monocytes and secrete γ-interferon, thereby contributing to vessel abnormalities[63]. Macrophages are also attracted by hypoxia, which in turn are inhibited by exosomes[64].

Microglia potentially participate in vascular pathology by enclosing and phagocytosing endothelial cells leading to blood vessel breakdown[65]. Hagberg *et al.*[66] reported that microglial cells exhibited dual actions in response to any brain insult; the first was excessive proinflammatory cytokine production and the second was anti-inflammatory agent production to limit injury.

Conversely, our exosome-treated group displayed downregulated Iba1 immune expression, IL-1β expression, and near-normal, field-free inflammatory cells. Consistent with our results, Kim *et al.*[67] reported that MSC-exosomes contained the anti-inflammatory mediator, α-1-anti-trypsin in the lung. MSC-derived EVs inhibited microglia activation and proinflammatory cytokine release by preventing Toll-like receptor-4 (TLR4)/CD14 signaling[68].

In our study, astrocytes were affected by increased BP; they appeared swollen with increased cytoplasm translucence and organelle loss. Astrocytes, in response to high BP, secrete IL-1β that stimulates an inflammation cascade[62], which further increases BBB permeability and elevates BP[69]. In contrast, astrocytes in exosome-administered rats exhibited near-normal structures helping in normalization of BBB. Nakano *et al.*[70] reported that bone marrow MSCs attenuated astrocyte impairment by transporting exosomal miR-146a into astrocytes in an Alzheimer's disease model. We also examined aquaporin 4 (AQP4), a membrane-bound protein in the perivascular end-feet of astrocytes that controls water flux. AQP4 expression was significantly increased in hypertensive rats. In contrast, exosome treatment decreased hypertension-induced AQP4 elevation, consistent with Khosrow Tayebati *et al.*[71]. AQP4 also regulates neural signal transduction and astrocyte migration[72].

Light and electron microscopy examinations of hypertensive animals showed degenerated apoptotic neuronal cells enclosed in a vacuolated neuropil. Immune histochemical results confirmed previous findings as evidenced by a significant increase in caspase 3 immune reactions. Furthermore, we observed a significant decline in Bcl-xl expression. Bcl-xl, one of the Bcl-2 groups of proteins, inhibits apoptosis via discrete mechanisms involving Bax inhibition[73]. Hypertension-induced neural loss in the brain can occur via the promotion of caspase-dependent apoptotic pathways and the inhibition of Bcl-2 and Bcl-xL survival pathways in the cerebral cortex[74]. Jalal *et al.*[75] attributed these insults to hypoperfusion, which occurs with hypertension or oxidative stress and destroys many cellular constituents especially neurons. Brown and Davis[76] suggested that neuronal apoptosis occurred from excess calcium entering neurons in response to oxidative stress. In a similar context, we assessed CB immune histochemical expression to evaluate neuronal damage and found that CB was significantly decreased in hypertensive rats. These findings were consistent with Denver *et al.*[77] who reported that CB staining reflected neuronal loss due to hypertension and Alzheimer's disease. Furthermore, these authors showed that increased caspase levels provoked a hyperinflammatory state by enhancing IL-1β via the TLR4 pathway.

We also observed myelin sheath separation. This phenomenon was explained by Brown *et al.*[78] as interstitial edema due to increased AQP4 levels, which eventually affect cerebral blood flow autoregulation[79]. This observation was consistent with our results as we observed increased AQP mRNA expression in hypertensive rats.

Importantly, nerve cells and fibers showed near-normal architecture in exosome-treated animals. A significant decrease in the immune expression of caspase 3 was also observed. The expression of Bcl-xl was also markedly enhanced. CB immune reactions showed a more robust increase. CB ensures neuroprotection by buffering intracellular calcium ion levels that inhibit different pro-apoptotic signaling pathways[80]. Similarly, Tan *et al.*[81] observed that hepatocyte proliferation occurred after exosome injection and was attributed to the stimulation of proliferating cell nuclear antigens and Bcl-xl. Zhang *et al.*[82] demonstrated that neuron growth occurred via the internalization of miRNA contents of exosomes into the degenerated neurons. We observed miRNA-133b (miR-133b) upregulation after exosome treatment in hypertensive rats. Other reports indicated that miR-133b transfer to nerve cells stimulated the growth of these cells[83], axonal density[27], and myelin regeneration[84]. Moreover, exosomes derived from MSCs contained miR-17 - 92, which stimulated neurogenesis and oligodendrocyte proliferation[85].

CONCLUSION

Hypertension initiates a cascade of events affecting cerebral tissues and blood vessels. Treatment with MSC-derived exosomes recovered

blood vessels, neural cells and BBB alterations as shown by extensive microscopy characterization. Exosome treatment stabilized blood vessels as shown by eNOS and AMPK mRNA upregulation and α-SMA mRNA downregulation, along with enhanced angiogenic factors, miRNA-222 and Tie2. Exosomes exerted anti-apoptotic effects by increasing Bcl-xl expression and decreasing caspase 3 protein levels. The anti-inflammatory potential of exosomes was endorsed by reductions in IL-1β mRNA and Iba1 protein levels. Neuronal protection was supported by miRNA-133b and CB protein upregulation. The astrocyte vascular feet protein, AQP4, was also downregulated, thereby restoring BBB integrity. In view of our observations, we propose MSC-derived exosomes as a novel strategy for treating cerebral hypertension complications. Nevertheless, further clinical trials and research in different tissues are warranted to explore their therapeutic efficacy and to verify their role as upcoming daily therapy.

The main limitation of the exosomal studies is the contamination with other types of EVs. This mainly relies on the method of isolation and characterization which can be improved by development in molecular profiling. Further, there are challenges in quantification of appropriate doses and uptake calculation.

CONFLICT OF INTEREST

There is no potential conflict of interest among the authors.

REFERENCES

1. Mills, K. T., Stefanescu, A., & He, J. (2020): The global epidemiology of hypertension. Nature Reviews Nephrology, 1 - 15.

2. Möller, K., Pösel, C., Kranz, A., Schulz, I., Scheibe, J., Didwischus, N., ... & Wagner, D. C. (2015): Arterial hypertension aggravates innate immune responses after experimental stroke. Frontiers in cellular neuroscience, 9, 461.

3. Thambisetty M, Biousse V, Newman NJ: (2003): Hypertensive brainstem encephalopathy: clinical and radiographic findings, 208:93–99.

4. Russo, E., Leo, A., Scicchitano, F., Donato, A., Ferlazzo, E., Gasparini, S., ... & Aguglia, U. (2017): Cerebral small vessel disease predisposes to temporal lobe epilepsy in spontaneously hypertensive rats. Brain Research Bulletin, 130, 245 - 250.

5. Kengne AP, Patel A, Barzi F, Jamrozik K, Lam TH, Ueshima H, Gu DF, Suh I, Woodward M. (2007): Systolic blood pressure, diabetes and the risk of cardiovascular diseases in the Asia-Pacific region. J Hypertens 25: 1205–1213.

6. James, P. A., Oparil, S., Carter, B. L., Cushman, W. C., Dennison-Himmelfarb, C., Handler, J., ... & Smith, S. C. (2014): 2014 evidence-based guideline for the management of high blood pressure in adults: report from the panel members appointed to the Eighth Joint National Committee (JNC 8). Jama, 311(5), 507 - 520.

7. Mohamed, E. M., Abdelrahman, S. A., Hussein, S., Shalaby, S. M., Mosaad, H., & Awad, A. M. (2017): Effect of human umbilical cord blood mesenchymal stem cells administered by intravenous or intravitreal routes on cryo-induced retinal injury. IUBMB life, 69(3), 188 - 201.

8. Khater, N. A., Selim, S. A., Abd El-Baset, S. A., & Abd El Hameed, S. H. (2017): Therapeutic effect of mesenchymal stem cells on experimentally induced hypertensive cardiomyopathy in adult albino rats. Ultrastructural Pathology, 41(1), 36 - 50.

9. Selim, S. A., Abd El-Baset, S. A., Kattaia, A. A., Askar, E. M., & Abd Elkader, E. (2019): Bone marrow-derived mesenchymal stem cells ameliorate liver injury in a rat model of sepsis by activating Nrf2 signaling. Histochemistry and cell biology, 151(3), 249 - 262.

10. Phinney, D. G., & Pittenger, M. F. (2017): Concise review: MSC-derived exosomes for cell-free therapy. Stem cells, 35(4), 851 - 858.

11. Jung JW, et al. (2013): Familial occurrence of pulmonary embolism after intravenous, adipose tissue-derived stem cell therapy. Yonsei Med J. ;54(5):1293 – 6.

12. Han, C.; Sun, X.; Liu, L.; Jiang, H.; Shen, Y.; Xu, X.; Li, J.; Zhang, G.; Huang, J.; Lin, Z.; et al. (2015): Exosomes and their therapeutic potentials of stem cells. Stem Cells Int. 2016, 1–11.

13. Yin, K., Wang, S., & Zhao, R. C. (2019): Exosomes from mesenchymal stem/stromal cells: a new therapeutic paradigm. Biomarker Research, 7(1), 8

14. Tsiapalis, D., and O'Driscoll, L. (2020): Mesenchymal stem cell derived extracellular vesicles for tissue engineering and regenerative medicine applications. Cells, 9(4), 991.

15. Tixeira, R., Caruso, S., Paone, S., Baxter, A. A., Atkin-Smith, G. K., Hulett, M. D., & Poon, I. K. (2017): Defining the morphologic features and products of cell disassembly during apoptosis. Apoptosis, 22(3), 475 - 477.

16. Surman, M., Hoja-Łukowicz, D., Szwed, S., Kędracka-Krok, S., Jankowska, U., Kurtyka, M., ... & Przybyło, M. (2019): An insight into the proteome of uveal melanoma-derived ectosomes reveals the presence of potentially useful biomarkers. International journal of molecular sciences, 20(15), 3789.

17. Gurunathan, S., Kang, M. H., Jeyaraj, M., Qasim, M., & Kim, J. H. (2019): Review of the isolation, characterization, biological function, and multifarious therapeutic approaches of exosomes. Cells, 8(4), 307.

18. Catalano, M.; O'Driscoll, L. (2019): Inhibiting extracellular vesicles formation and release: a review of EV inhibitors. J. Extracell. Vesicles, 9, 1703244.

19. Pfeifer, P.; Werner, N.; Jansen, F. (2015): Role and function of microRNAs in extracellular vesicles in cardiovascular biology. BioMed Res. Int. 2015, 1–11.

20. Valadi H, Ekström K, Bossios A, Sjöstrand M, Lee JJ, Lötvall JO. (2007): Exosome-mediated transfer of mRNAs and microRNAs is a novel mechanism of genetic exchange between cells. Nat Cell Biol.; 9: 654–9.

21. Li, Q., Yon, J. Y., & Cai, H. (2015): Mechanisms and consequences of eNOS dysfunction in hypertension. Journal of hypertension, 33(6), 1128.

22. Bian, S.; Zhang, L.; Duan, L.; Wang, X.; Min, Y.; Yu, H. (2013): Extracellular vesicles derived from human bone marrow mesenchymal stem cells promote angiogenesis in a rat myocardial infarction model. J. Mol. Med., 92, 387–397.

23. Sengupta, V., Sengupta, S., Lazo, A., Woods, P., Nolan, A., & Bremer, N. (2020): Exosomes derived from bone marrow mesenchymal stem cells as treatment for severe COVID-19. Stem Cells and Development.

24. Chen, H. X., Liang, F. C., Gu, P., Xu, B. L., Xu, H. J., Wang, W. T., ... & An, S. J. (2020): Exosomes derived from mesenchymal stem cells repair a Parkinson's disease model by inducing autophagy. Cell Death & Disease, 11(4), 1 - 17.

25. Takata, K.; Matsuzaki, T.; Tajika, Y.; Ablimit, A.; Hasegawa, T. (2008): Localization and trafficking of aquaporin 2 in the kidney. Histochem. Cell Biol. 2, 197–209.

26. Lai, R.C.; Yeo, R.W.; Tan, K.H.; Lim, S.K. (2013): Exosomes for drug delivery—A novel application for the mesenchymal stem cell. Biotechnol. Adv. 5, 543–551.

27. Xin, H., Li, Y., Cui, Y., Yang, J. J., Zhang, Z. G., & Chopp, M. (2013): Systemic administration of exosomes released from mesenchymal stromal cells promote functional recovery and neurovascular plasticity after stroke in rats. Journal of Cerebral Blood Flow & Metabolism, 33(11), 1711 - 1715.

28. Chelko, S. P., Schmiedt, C. W., Lewis, T. H., Lewis, S. J., & Robertson, T. P. (2012): A novel vascular clip design for the reliable induction of 2-kidney, 1-clip hypertension in the rat. Journal of applied physiology, 112(3), 362 - 366.

29. Faruk EM, El Sawy NA. (2015): Histological, immunohistochemical and biochemical study on the possible cardioprotective and antihypertensive role of the flavonoid in unilateral renal artery ligation of adult albino rats. J Cytol Histol.;2015.

30. Thery C, Amigorena S, Raposo G, Clayton A. (2006): Isolation and characterization of exosomes from cell culture supernatants and biological fluids. Curr. Protoc. Cell Biol. 2006;Chapter 3:Unit 3.22.

31. Bhatnagar S, Schorey JS. (2007): Exosomes released from infected macrophages contain mycobacterium avium glycopeptidolipids and are proinflammatory. J Biol Chem.; 282: 25779–25789.

32. Dominkuš, P. P., Stenovec, M., Sitar, S., Lasič, E., Zorec, R., Plemenitaš, A., ... & Lenassi, M. (2018): PKH26 labeling of extracellular vesicles: Characterization and cellular internalization of contaminating PKH26 nanoparticles. Biochimica et Biophysica Acta (BBA)-Biomembranes, 1860(6), 1350 - 1361.

33. Li, D., Zhang, P., Yao, X., Li, H., Shen, H., Li, X., ... & Lu, X. (2018): Exosomes derived from miR-133b-modified mesenchymal stem cells promote recovery after spinal cord injury. Frontiers in neuroscience, 12, 845.

34. Hutter-Schmid, B., Kniewallner, K. M., & Humpel, C. (2015): Organotypic brain slice cultures as a model to study angiogenesis of brain vessels. Frontiers in cell and developmental biology, 3, 52.

35. Kiernan, J. A. (2000): Histological and Histochemical Methods: Theory and Practice 3rd edn. (Hodder Arnold Publishers, 2000).

36. Ramos-Vara, J. A., Kiupel, M., Baszler, T., Bliven, L., Brodersen, B., Chelack, B., ... & West, K. (2008): American association of veterinary laboratory diagnosticians subcommittee on standardization of immunohistochemistry suggested guidelines for immunohistochemical techniques in veterinary diagnostic laboratories. J. Vet. Diagn. Invest. 20(4), 393–413 (2008).

37. Ayache, J., Beaunier, L., Boumendil, J., Ehret, G., & Laub, D. (2010): Sample Preparation Handbook for Transmission Electron Microscopy:Techniques. Vol. 2. (Springer, 2010).

38. Margolis, L., & Sadovsky, Y. (2019): The biology of extracellular vesicles: The known unknowns. PLoS biology, 17(7), e3000363.

39. Rapoport SI (2000): Osmotic opening of the blood brain barrier: principles, mechanisms and therapeutic application. Cell Mol Neurobiol 20:217.

40. de la Torre JC (2000): Critically attained threshold of cerebral hypoperfusion: the CATCH hypothesis of Alzheimer's pathogenesis. Neurobiol Aging 21:331–42.

41. Katusic, Z. S., & Austin, S. A. (2014): Endothelial nitric oxide: protector of a healthy mind. European heart journal, 35(14), 888 - 894.

42. Wang, F., Cao, Y., Ma, L., Pei, H., Rausch, W. D., & Li, H. (2018): Dysfunction of cerebrovascular endothelial cells: prelude to vascular dementia. Frontiers in aging neuroscience, 10, 376.

43. Claret, M., Smith, M. A., Batterham, R. L., Selman, C., Choudhury, A. I., Fryer, L. G., ... & Withers, D. J. (2007): AMPK is essential for energy homeostasis regulation and glucose sensing by POMC and AgRP neurons. The Journal of clinical investigation, 117(8), 2325 - 2336.

44. Mair, W., Morantte, I., Rodrigues, A. P., Manning, G., Montminy, M., Shaw, R. J., & Dillin, A. (2011): Lifespan extension induced by AMPK and calcineurin is mediated by CRTC-1 and CREB. Nature, 470(7334), 404 - 408.

45. Xu, Q., & Si, L. Y. (2010): Protective effects of AMP-activated protein kinase in the cardiovascular system. Journal of cellular and molecular medicine, 14(11), 2604.2613-

46. Attwell, D., Mishra, A., Hall, C. N., O'Farrell, F. M., & Dalkara, T. (2016): What is a pericyte? Journal of Cerebral Blood Flow & Metabolism, 36(2), 451 - 455.

47. Hutter-Schmid, B., & Humpel, C. (2016): Alpha-smooth muscle actin mRNA and protein are increased in isolated brain vessel extracts of Alzheimer mice. Pharmacology, 98(5- 6), 251 - 260.

48. Iadecola C and Davisson RL. (2008): Hypertension and cerebrovascular dysfunction. Cell Metab 7: 476 – 484.

49. Feng, R., Ullah, M., Chen, K., Ali, Q., Lin, Y., & Sun, Z. (2020): Stem cell-derived extracellular vesicles mitigate ageing-associated arterial stiffness and hypertension. Journal of extracellular vesicles, 9(1), 1783869.

50. Atienzar-Aroca, S.; Flores-Bellver, M.; Serrano-Heras, G.; Martinez-Gil, N.; Barcia, J.M.; Aparicio, S.; Perez-Cremades, D.; Garcia-Verdugo, J.M.; Diaz-Llopis, M.; Romero, F.J.; et al. (2016): Oxidative stress in retinal pigment epithelium cells increases exosome secretion and promotes angiogenesis in endothelial cells. J. Cell Mol. Med. 20, 1457–1466.

51. Yang, Y., Cai, Y., Zhang, Y., Liu, J., & Xu, Z. (2018): Exosomes secreted by adipose-derived stem cells contribute to angiogenesis of brain microvascular endothelial cells following oxygen–glucose deprivation in vitro through microRNA-181b/TRPM7 axis. Journal of Molecular Neuroscience, 65(1), 74 - 83.

52. Jones N, Iljin K, Dumont DJ, Alitalo K. (2001): Tie receptors: new modulators of angiogenic and lymphangiogenic responses. Nat Rev Mol Cell Biol 2001; 2: 257–67.

53. Takahara K, Iioka T, Furukawa K, Uchida T, Nakashima M, Tsukazaki T, Shindo H. (2004): Autocrine/paracrine role of the angiopoietin-1 and -2/Tie2 system in cell proliferation and chemotaxis of cultured fibroblastic synoviocytes in rheumatoid arthritis. Hum Pathol. 2004; 35: 150–8.

54. Kosacka J, Figiel M, Engele J, Hilbig H, Majewski M, Spanel-Borowski K. (2005): Angiopoietin-1 promotes neurite outgrowth from dorsal root ganglion cells positive for Tie-2 receptor. Cell Tissue Res. 2005; 320: 11–9.

55. Zhao YD, Campbell AI, Robb M, Ng D, Stewart DJ. (2003): Protective role of angiopoietin-1 in

experimental pulmonary hypertension. Circ Res 2003; 92:984–991.

56. Yamamoto, A., Takahashi, H., Kojima, Y., Tsuda, Y., Morio, Y., Muramatsu, M., & Fukuchi, Y. (2008): Downregulation of angiopoietin-1 and Tie2 in chronic hypoxic pulmonary hypertension. Respiration, 75(3), 328 - 338.

57. Zhao, T., Yan, Z., Liu, J., Sun, H., Chen, Y., Tao, Y., ... & Yan, Y. (2018): Mesenchymal stem cell derived exosomes enhance lymphangiogenesis via exosomal transfer of Ang-2/Tie2. BioRxiv, 466987.

58. Wysoczynski M, Pathan A, Moore JB, Farid T, Kim J, Nasr M, Kang Y, Li H,Bolli R. (2019): Pro-Angiogenic actions of CMC-derived extracellular vesicles rely on selective packaging of Angiopoietin 1 and 2, but not FGF-2 and VEGF. Stem Cell Rev Rep. 2019;15:530–42.

59. Ward NL, Putoczki T, Mearow K, Ivanco TL, Dumont DJ. (2005): Vascular-specific growth factor angiopoietin 1 is involved in the organization of neuronal processes. J Comp Neurol. 2005; 482: 244–56.

60. Pires, P. W., Dams Ramos, C. M., Matin, N., & Dorrance, A. M. (2013): The effects of hypertension on the cerebral circulation. American Journal of Physiology-Heart and Circulatory Physiology, 304(12), H1598-H1614.

61. Ohsawa, K., Imai, Y., Sasaki, Y., & Kohsaka, S. (2004): Microglia/macrophage-specific protein Iba1 binds to fimbrin and enhances its actin-bundling activity. Journal of neurochemistry, 88(4), 844 - 856.

62. Kaiser, D., Weise, G., Moller, K., Scheibe, J., Posel, C., Baasch, S., et al. (2014): Spontaneous white matter damage, cognitive decline and neuroinflammation in middle-aged hypertensive rats: an animal model of early-stage cerebral small vessel disease. Acta Neuropathol. Commun. 2:169.

63. Kossmann S, Schwenk M, Hausding M, Karbach SH, Schmidgen MI, Brandt M, Knorr M, Hu H, Kroller-Schon S, Schonfelder T, Grabbe S, Oelze M, Daiber A, Munzel T, Becker C, Wenzel P (2013): Angiotensin II-induced vascular dysfunction depends on interferon-gamma-driven immune cell recruitment and mutual activation of monocytes and NK-cells. Arterioscler Thromb Vasc Biol 33(6):1313? 1319.

64. Lee C, Mitsialis SA, Aslam M, Vitali SH, Vergadi E, Konstantinou G, et al. (2012): Exosomes mediate the cytoprotective action of mesenchymal stromal cells on hypoxia-induced pulmonary hypertension. Circulation. 126:2601–11.

65. Jolivel, V., Bicker, F., Binamé, F., Ploen, R., Keller, S., Gollan, R., ... & Schmidt, M. H. (2015): Perivascular microglia promote blood vessel disintegration in the ischemic penumbra. Acta neuropathologica, 129(2), 279 - 295.

66. Hagberg H, Mallard C, Ferriero DM, Vannucci SJ, Levison SW, Vexler ZS, et al. (2015): The role of inflammation in perinatal brain injury. Nat Rev Neurol; 11: 192–208.

67. Kim, Y. S., Kim, J. Y., Cho, R., Shin, D. M., Lee, S. W., & Oh, Y. M. (2017): Adipose stem cell-derived nanovesicles inhibit emphysema primarily via an FGF2-dependent pathway. Experimental & Molecular Medicine, 49(1), e284.

68. Thomi, G., Surbek, D., Haesler, V., Joerger-Messerli, M., & Schoeberlein, A. (2019): Exosomes derived from umbilical cord mesenchymal stem cells reduce microglia-mediated neuroinflammation in perinatal brain injury. Stem cell research & therapy, 10(1), 105.

69. Shi, P., Diez-Freire, C., Jun, J. Y., Qi, Y., Katovich, M. J., Li, Q., ... & Raizada, M. K. (2010): Brain microglial cytokines in neurogenic hypertension. Hypertension, 56(2), 297 - 303.

70. Nakano, M., Kubota, K., Kobayashi, E., Chikenji, T. S., Saito, Y., Konari, N., & Fujimiya, M. (2020): Bone marrow-derived mesenchymal stem cells improve cognitive impairment in an Alzheimer's disease model by increasing the expression of microRNA-146a in hippocampus. Scientific reports, 10(1), 1 - 15.

71. Khosrow Tayebati, S., Amenta, F., & Tomassoni, D. (2015): Cerebrovascular and blood-brain barrier morphology in spontaneously hypertensive rats: effect of treatment with choline alphoscerate. CNS & Neurological Disorders-Drug Targets (Formerly Current Drug Targets-CNS & Neurological Disorders), 14(3), 421 - 429.

72. Kimelberg, H. K., & Nedergaard, M. (2010): Functions of astrocytes and their potential as therapeutic targets. Neurotherapeutics, 7(4), 338 - 353.

73. Stevens, M., & Oltean, S. (2019): Modulation of the apoptosis gene Bcl-x function through alternative splicing. Frontiers in genetics, 10, 804.

74. Li, Y., Liu, J., Gao, D., Wei, J., Yuan, H., Niu, X., & Zhang, Q. (2016): Age related changes in hypertensive brain damage in the hippocampi of spontaneously hypertensive rats. Molecular medicine reports, 13(3), 2552 - 2560.

75. Jalal, F. Y., Yang, Y., Thompson, J., Lopez, A. C., & Rosenberg, G. A. (2012): Myelin loss associated with neuroinflammation in hypertensive rats. Stroke, 43(4), 1115 - 1122.

76. Brown RC and Davis TP (2002): Calcium modulation of adherens and tight junctions function. Stroke 33:1706–11.

77. Denver, P., D'Adamo, H., Hu, S., Zuo, X., Zhu, C., Okuma, C., ... & Frautschy, S. A. (2019): A novel model of mixed vascular dementia incorporating hypertension in a rat model of Alzheimer's disease. Frontiers in physiology, 10, 1269.

78. Brown, C. A., Munday, J. S., Mathur, S., & Brown, S. A. (2005): Hypertensive encephalopathy in cats with reduced renal function. Veterinary pathology, 42(5), 642 - 649.

79. Tayebati, S. K., Tomassoni, D., & Amenta, F. (2012): Spontaneously hypertensive rat as a model of vascular brain disorder: microanatomy, neurochemistry and behavior. Journal of the neurological sciences, 322(1 - 2), 241 -249.

80. Kook, S.Y.; Jeong, H.; Kang, M.J.; Park, R.; Shin, H.J.; Han, S.H.; et al. (2014): Crucial role of calbindin-D 28k in the pathogenesis of Alzheimer's disease mouse model. Cell Death Differ. 21(10), 1575 - 87.

81. Tan CY, et al. (2014): Mesenchymal stem cell-derived exosomes promote hepatic regeneration in drug-induced liver injury models. Stem Cell Res Ther. 5(3):76.

82. Zhang, Y.; Chopp, M.; Liu, X.S.; Katakowski, M.; Wang, X.; Tian, X.; Wu, D.; Zhang, Z.G. (2017): Exosomes Derived from Mesenchymal Stromal Cells Promote Axonal Growth of Cortical Neurons. Mol. Neurobiol. 54, 2659–2673.

83. Xin, H., Li, Y. I., Buller, B., Katakowski, M., Zhang, Y., Wang, X., ... & Chopp, M. (2012): Exosome-mediated transfer of miR-133b from multipotent mesenchymal stromal cells to neural cells contributes to neurite outgrowth. Stem cells, 30(7), 1556 - 1564.

84. Clark, K.; Zhang, S.; Barthe, S.; Kumar, P.; Pivetti, C.D.; Kreutzberg, N.; Reed, C.; Wang, Y.; Paxton, Z.J.; Farmer, D.L.; et al. (2019): Placental mesenchymal stem cell-derived extracellular vesicles promote myelin regeneration in an animal model of multiple sclerosis. Cells 8, 1497.

85. Xin H, et al. (2017): MicroRNA cluster miR-17-92 cluster in exosomes enhance neuroplasticity and functional recovery after stroke in rats. Stroke. 48(3):747–53.